International Journal of Engineering Trends and Technology
ISSN: 2231 – 5381 / https://doi.org/10.14445/22315381/IJETT-V70I5P215

Volume 70 Issue 5, 120-130, May 2022

Original Article

The Adequate Exploitation of Grid-Connected Single-Phase Photovoltaic Systems Unceasingly

CH Venkata Ramesh[1], A Manjunatha[2]

[1] *Department of E&EE, NMIT, Bangalore, Karnataka, India*
[2] *Department of E&EE, SKIT, Bangalore, India.*

[1] cvram256@gmail.com

Received: 08 February 2022 Revised: 31 March 2022 Accepted: 07 April 2022 Published: 19 May 2022

Abstract - *Many countries are converting to renewable energy sources as the cost of grid electricity has risen dramatically. A DC-DC converter and a DC-AC converter are typically needed to link a solar photovoltaic system to the grid, and this is referred to as a double-stage conversion system. This proposed double-stage solar photovoltaic system adopts the suggested approach to deliver actual power and adjusts with the reactive power of the load. To further utilize the capacity of the voltage source inverter, a reactive power compensation operation is envisaged when there is no photovoltaic generation. The simulated results describe and demonstrate the multifunctional properties of the proposed methodology.*

Keywords - *Maximum power point (MPP), Reactive power compensation, Solar photovoltaic system, Voltage source inverter.*

1. Introduction

Solar photovoltaic technology advances and is implemented in grid-connected systems. Solar photovoltaics are an appealing option for generating environmentally benign power for various uses [1]. Solar photovoltaic energy is now widely employed in distributed generation systems. To deliver the most electricity to the grid, grid-connected solar PV systems must operate at their MPP [2]. Due to their simplicity and availability, the standard voltage source inverter and harmonic filter are the most utilized interface units in grid-connected solar photovoltaic system technology [3].

It is popular to use dual- and single-stage solar photovoltaic system topologies associated with the grid in single-phase power grids. This design includes two steps: a DC-DC conversion step and a DC-AC inverter step to connect the solar photovoltaic system to the grid, respectively [4] and [5]. In [6], an ANFIS-based solar PV system connected to the grid for voltage control is proposed. [7] implements a single-stage solar PV and energy storage system management based on a household electricity price. Due to its low efficiency and higher cost, the one-step technique is not appealing to network-connected systems that need to be efficient. But when comparing efficiency, the double stage architecture has become increasingly popular in low voltage applications since it is more efficient than the one-stage conversion method. In [8], [9], a comparison of the various interface units for two-stage topologies is offered. In [10], [11], and [12], [13], [14] a more efficient two-stage solar system connected to the network is detailed. However, the absence of neutral current adjustment will increase the percent THD of grid current. The solar photovoltaic system is based on a dual conversion unit to track MPP and connect to the grid in a dual-stage system linked to the electrical grid. With this design, the most solar photovoltaic power is given to the network in the most efficient, smallest, and cheapest way possible.

Grid-connected solar photovoltaic systems have improved conversion efficiency, but they still face intermittent power generation and dynamic energy demand. Solar PV systems connected to the network can benefit from the addition of an energy storage system [15], [16] [17]. The literature [18], [19], and [20] investigate grid-connected solar PV energy management with energy storage. On the other hand, these systems use hybrid energy storage devices; two-step electric conversion is carried out in these systems. In [21], hybrid energy management and control storage system has been introduced for various modes of operation. A reconfigurable one-stage photovoltaic (PV) and a battery-powered solar converter system has been developed [22], [23], [24], [25]. In this case, the peak power point can only be accomplished while the battery is being charged or when electricity is being injected into the grid, but not both at the same time.

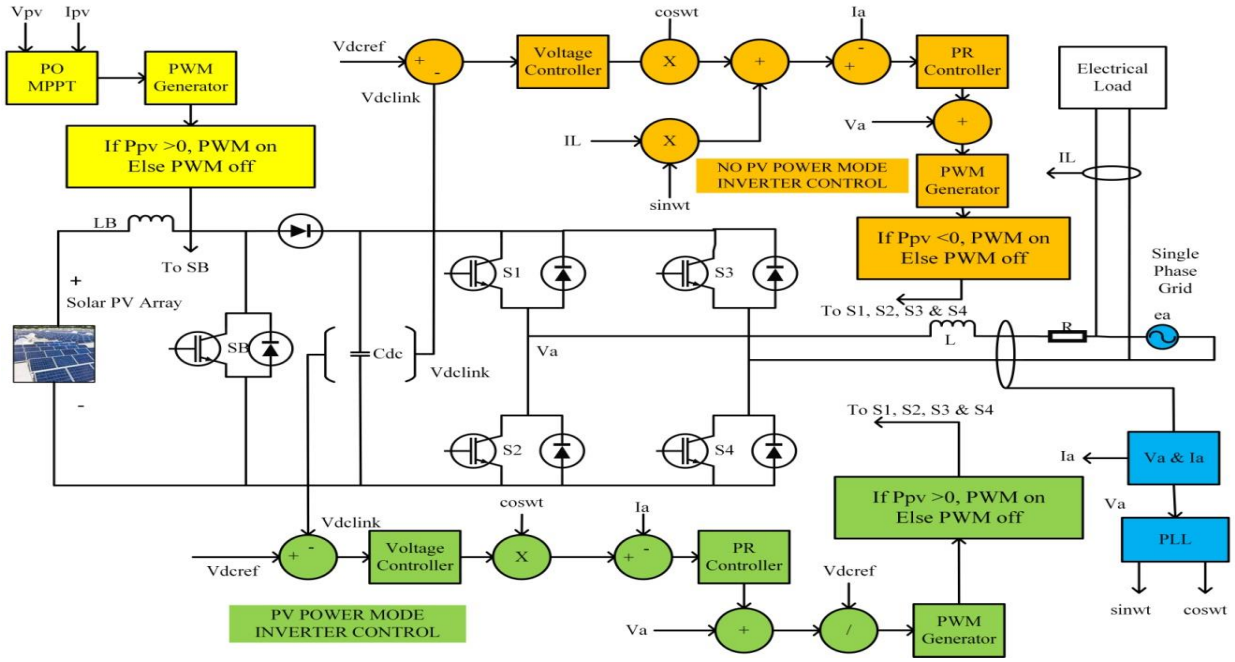

Fig. 1The grid-connected solar photovoltaic system in a single-phase network

The proposed solar photovoltaic grid-connected system will operate with multiple functions in this work. Depending on the amount of solar PV energy available, the suggested control operation has two different working modes: 1) PV Power Mode and 2) No PV Power Mode. The organization document is as follows; the system's functioning under consideration is described in Section 2. The suggested system's architecture can be found in Section 3. The results of the simulation and their analysis are discussed in Section 4. The planned work's conclusions are presented in Section 5.

2. The solar PV system is connected to the grid with real and reactive output control.

A dual-controlled grid-connected solar PV system in a single-phase network is presented in figure 1. The photovoltaic modules are combined in series and in parallel to meet the voltage and supply requirements of the solar photovoltaic network. The DC-DC converter is controlled via a power peak tracking algorithm to track the peak of solar photovoltaic power. Two loops that control the voltage source inverter are i) the outer loop used for voltage control of the DC link and ii) the internal loop used for current control in PV mode. Additionally, the voltage source inverter offers reactive power compensation, current balancing, and active rectification, enhancing the power factor during the No PV power mode.

During PV power mode, PV voltage (Vpv) and current (Ipv) are measured in the PV panel, and it is processed via peak power tracking algorithm, i.e., perturb & observe method. The peak power monitoring algorithm provides an operating cycle for the PWM generator. The PWM generator controls the electronic power switch in the Boost converter to get the most out of the PV system's peak power. The dc-link capacitor voltage (Vdclink) is measured and compared to the dc-link reference voltage (Vdcref). This error voltage is processed via the proportional-integral controller. The proportional-integral controller generates the reference peak current for the voltage source inverter. The reference peak current and cos(ωt) product is compared with the inverter current. The error current is processed through the proportional resonant controller, generating the control voltage. It is added to the grid voltage and passed via a sinusoidal PWM generator. The sinusoidal PWM generator generates the pulse for a single-phase inverter to supply the grid with real power during PV power mode.

During No PV power mode, the switching signal concerning the DC-DC boost converter is cut off and disconnected from the system. During this mode, dc-link voltage (Vdclink) and dc-link reference voltage (Vdcref) are processed via a proportional-integral controller, and it generates peak current reference current. The reference peak current and cos(ωt) product is added to $I_L\sin(\omega t)$. This current is compared with inverter current (Ia) and processed through a proportional resonant controller. The proportional resonant controller output is added with grid voltage and processed via a sinusoidal PWM generator. The sinusoidal PWM generator generates the switching pulse for a single-phase inverter to deliver reactive power to the load.

3. Solar PV system design for single-phase grid connection

The solar PV array is created by connecting the panels in series and parallel. The rating of the single PV panel is 349.59 W, 43 V, 8.13 A. six-panel is connected in series to build up the voltage around 258 V. the total rating of the solar PV array is 2097.54 W, 258 V &8.13 A. For various irradiance circumstances, the Current vs. Voltage and Power vs. Voltage features of the proposed solar PV array are presented in figure 2. The Simulink model of a grid-connected solar PV system is presented in figure 3.

The DC-DC power converter is sized to match the output of photovoltaic solar panels.

The DC-DC power converter is sized to match the output of photovoltaic solar panels. The input voltage of the boost converter is 258 volts, while the output voltage of the DC-DC boost converter is 400 V. The DC-DC boost converter's maximum output current is 5.25 A. The boost converter's inductor value is 20 mH for a 2 % ripple inductor current. The capacitor value of the boost converter for the 2 % ripple capacitor voltage is 3000 µF.

3.1. LCL filter design for grid-connected solar photovoltaic inverter

To integrate solar PV into the grid, the harmonic filter is crucial. The LCL (Inductor-Capacitor-Inductor) filters between the inverter and grid as presented in figure 4.

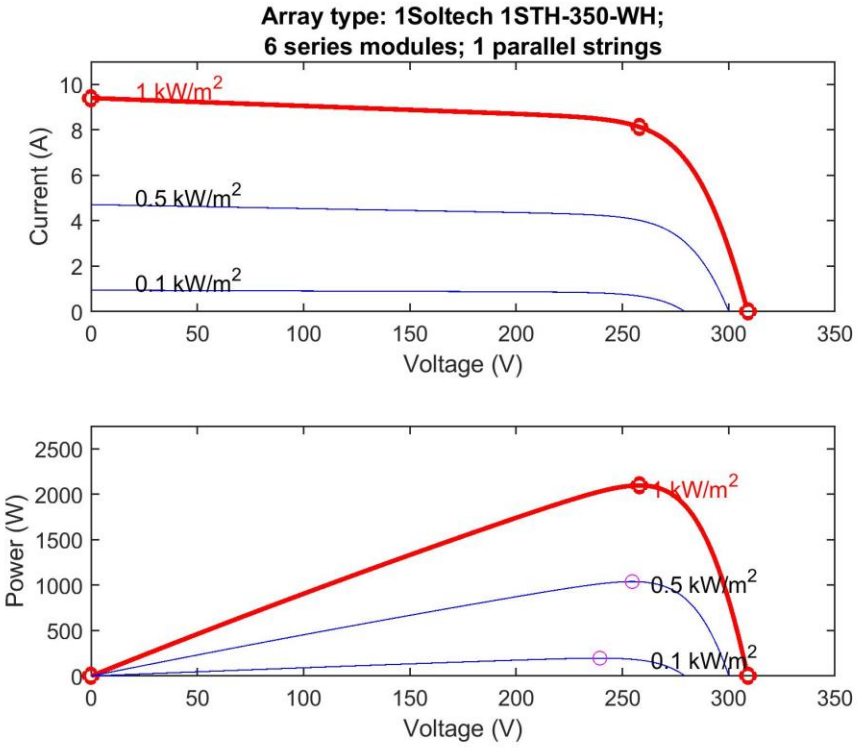

Fig. 2 The solar PV array's Current vs. Voltage and Power vs. Voltage characteristics.

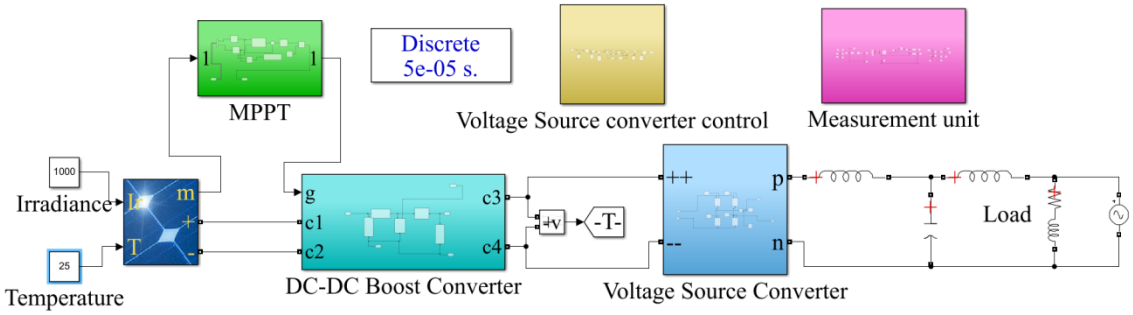

Fig. 3 Simulink model of a grid-connected solar PV system.

The filter design is depicted in this section. Equations (1) and (2) give the system's base impedance and base capacitance.

$$Z_{base} = \frac{V_{ph}^2}{P} \qquad (1)$$

$$C_{base} = \frac{1}{\omega_n * Z_{base}} \qquad (2)$$

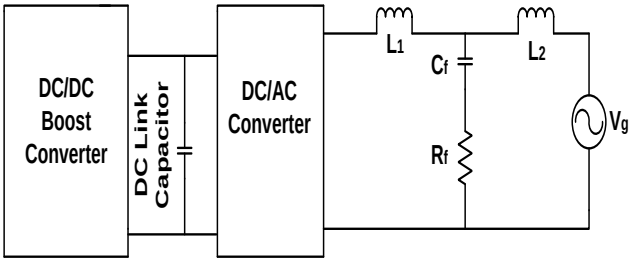

Fig. 4 Block diagram of the grid-connected PV inverter with LCL filter.

Where Z_{base} is base impedance and C_{base} is base capacitance. Vph represents phase voltage, P is the rated active power, and ω_n is the nominal angular frequency. The value of the filter capacitor is selected based on the base capacitance of the system and is given in the equation (3).

$$C_f = \frac{C_{base}}{2} \qquad (3)$$

Equation (4) gives the maximum current ripple considering 20% of the maximum current.

$$\Delta I_{max} = 0.2 * I_{max} \qquad (4)$$

Where I_{max} is given in equation (5).

$$I_{max} = \frac{S_{rated} * \sqrt{2}}{V_{ph}} \qquad (5)$$

The filter inductances L_1 and L_2 are given in Equations (6) and (7).

$$L_1 = \frac{V_{DC}}{4 * f_{SW} * \Delta I_{max}} \qquad (6)$$

Where L1 is Inverter-side filter inductance, f_{SW} is inverter switching frequency, and V_{DC} is DC-link voltage.

$$L_1 + L_2 = \frac{0.1 * V_{ph}^2}{S * 2 * pi * f_g} \qquad (7)$$

L2 is grid-side filter inductance, f_g is frequency, and V_{ph} is grid voltage.

$$f_r = \frac{1}{2\pi} * \sqrt{\frac{L_1 + L_2}{L_1 * L_2 * C_f}} \qquad (8)$$

The capacitor should be linked in series with a resistor to decrease oscillations and unstable states of the filter. Passive damping is a term used to describe this solution. It's easy and dependable, but it raises the system's heat losses and significantly reduces the filter's effectiveness. The following formula can be used to calculate the value of the damping resistor:

$$R_f = \frac{1}{3 * \omega_R * C_f} \qquad (9)$$

Table 1 represents the parameters of the LCL filter.

Table 1. Parameters of the LCL filter

Parameter	Value
Grid voltage(V_{ph})	230 V
The output power of the inverter(*S_{rated}*)	2000 VA
DC-Link voltage	400 V
Grid frequency	50 Hz
Switching frequency	15 kHz
Inverter-side inductor *L_1*	2.7 mH
Grid-side inductor *L_2*	5.71 mH
Filter capacitor *C_f*	6.01 µF
Damping resistor *R_f*	5.8274Ω
Resonance frequency(f_r)	1513Hz

3.2. PR Controller for grid-connected solar photovoltaic inverter

The model of the PR control is presented in Figure 5.

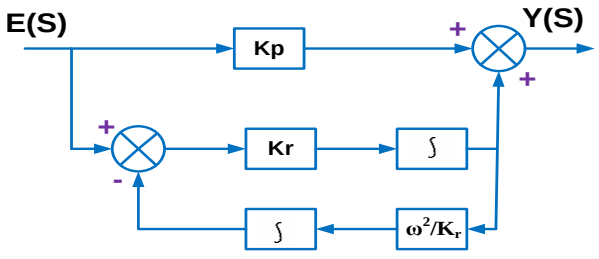

Fig. 5 Model of PR controller

The following (10) is the best way to describe a PR controller's transfer function:

$$G_{PR}(S) = K_P + \frac{2 * K_r * S}{S^2 + \omega_o^2} \qquad (10)$$

The proportional and resonance gains, respectively, are Kp and Kr. Like a PI controller, Kr is in charge of removing steady-state error while Kp is set to provide good transient response and stability [26].

The unlimited gain associated with the ideal scenario may cause instability issues in practice. To increase the performance of the managed system, a non-ideal PR controller, as described in [27], can be used:

$$G_{PR}(S) = K_P + \frac{2 * \omega_c * K_r * S}{S^2 + 2 * \omega_c * S + \omega_O^2} \qquad (11)$$

The controller's parameters are listed in Table 2.

Table 2. Parameters of the PR controller

Parameter	Value
Proportional gain *(Kp)*	8.5
Resonant gain *(Kr)*	100

4. Discussion of simulation findings

The proposed single-phase grid-connected solar PV system is created in the MATLAB Simulink software. The Simulink model of the single-phase grid-connected solar PV system is demonstrated in Figure3. The proposed model is tested in two modes such as PV power mode and No PV Power mode. Constant irradiance, varying irradiance, and varying temperature conditions are considered in the PV power mode. No PV power mode reactive load is connected to the system, and corresponding results are analyzed.

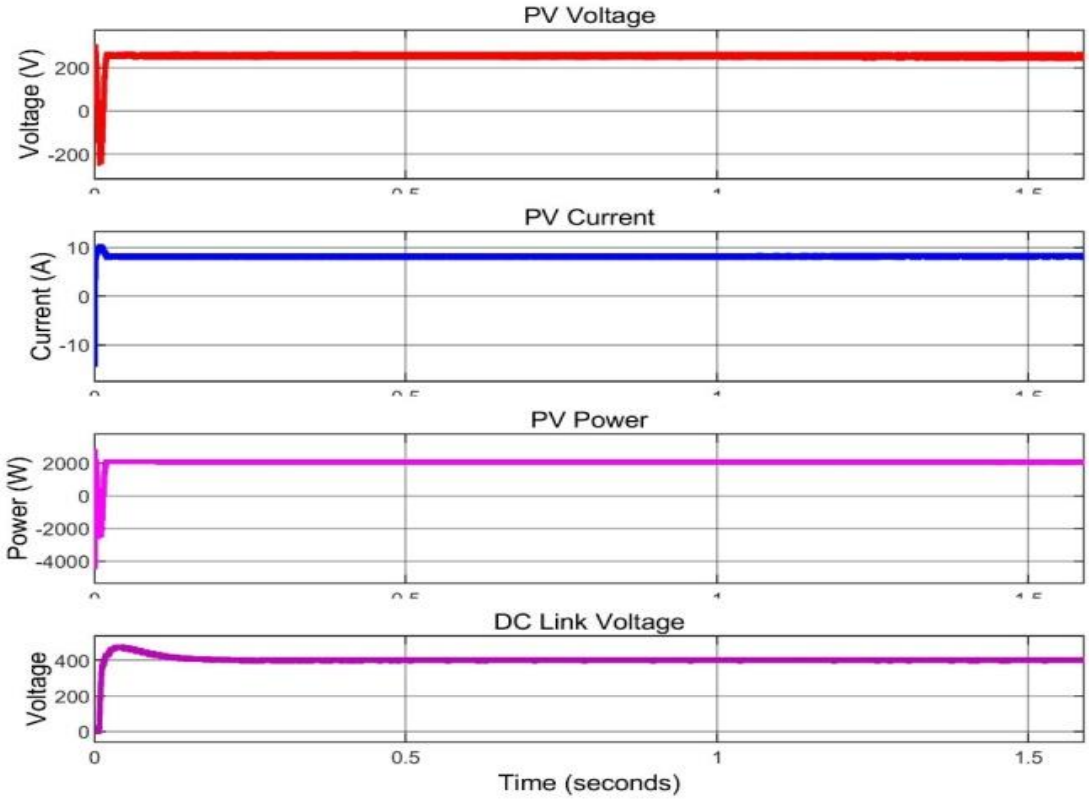

(a)

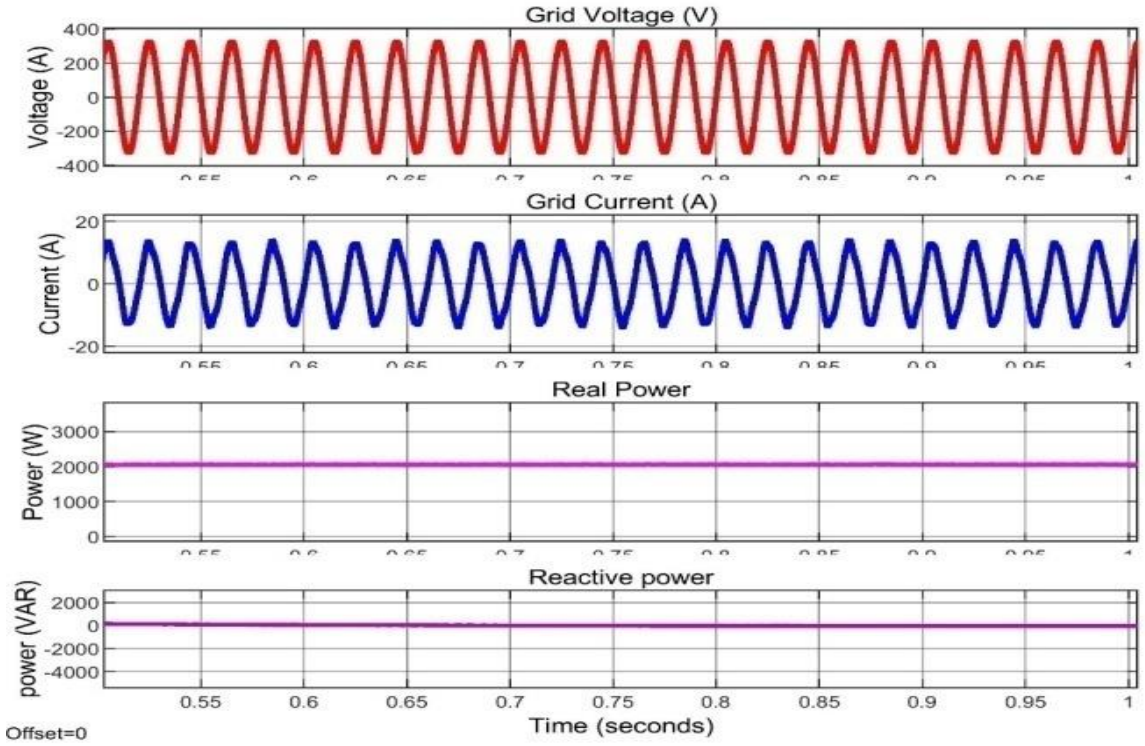

(b)

Fig. 6 Simulation results for constant irradiance at 1000 W/m2: a) PV voltage, current, power, and dc-link voltage, b) Grid voltage, current, real power, and reactive power.

In constant irradiance conditions, irradiance and temperature are kept at 1000 W/m2 and 25^0 C, and corresponding results such as PV Voltage, PV Current, PV power, grid voltage, grid current, grid power, and dc-link voltage are measured and analyzed (Figure 6).

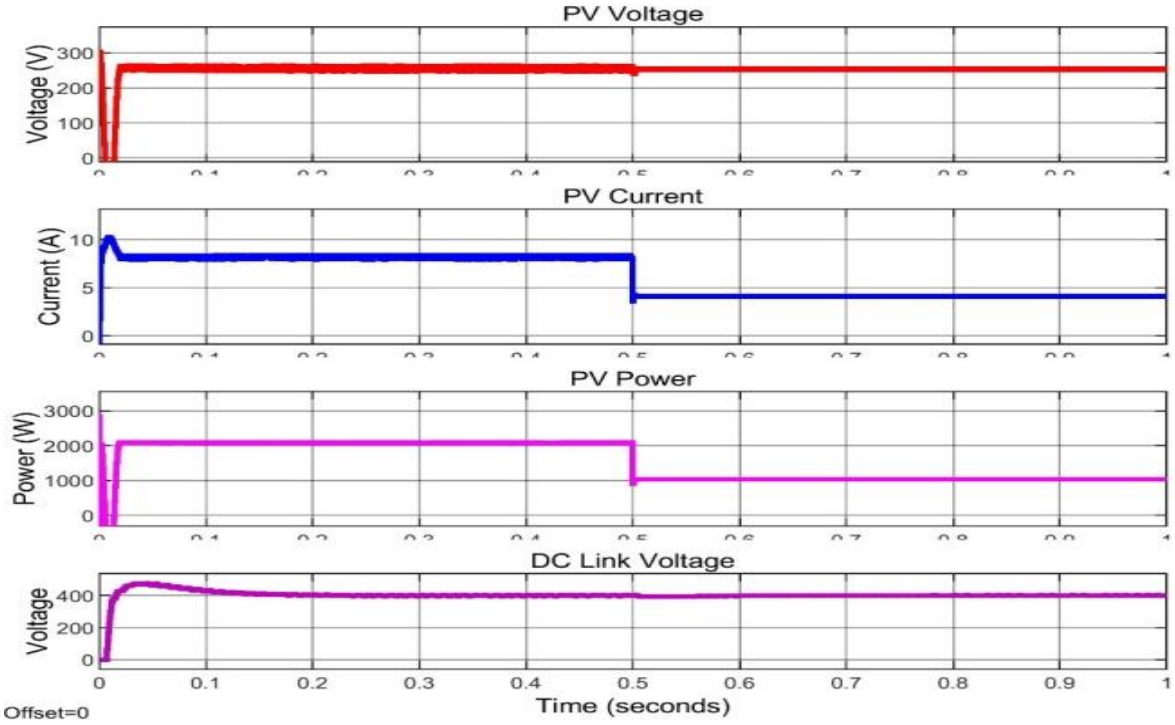

(a)

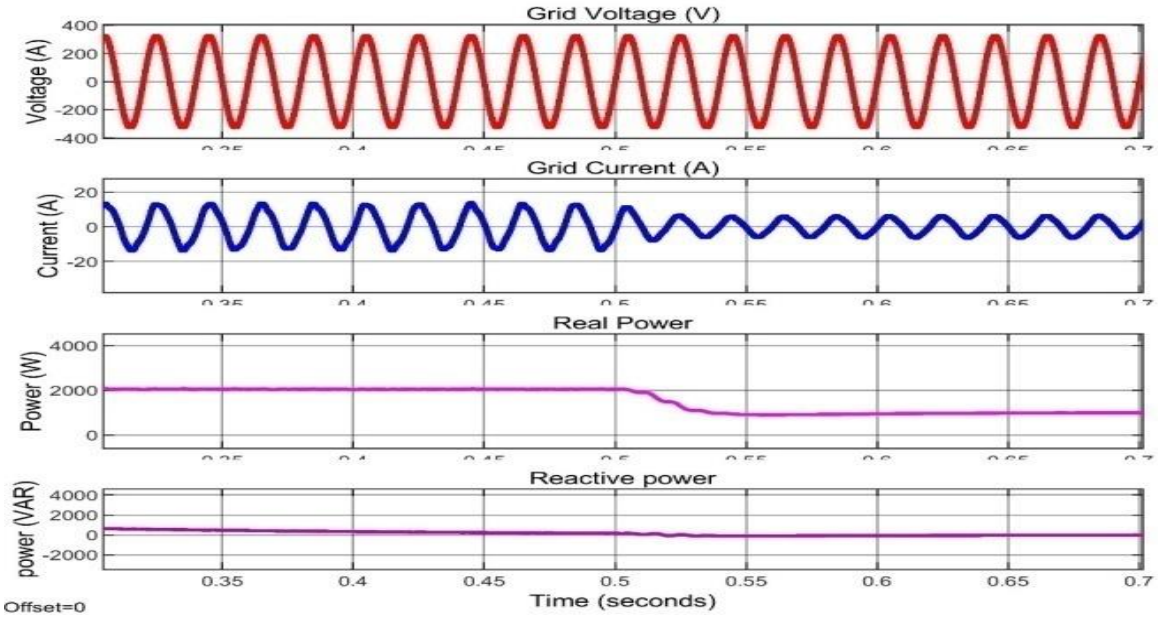

(b)

Fig. 7 Simulation results for varying irradiance from 1 kW/m^2 to 0.5 kW/m^2 at 0.5 sec: a) PV voltage, current, power, and dc-link voltage, b) Grid voltage, current, real power, and reactive power.

From figure 7, it is observed that power generation from PV array is around 2095 W, PV panel is around 259 V, and PV current is around 8.08 A. The voltage at the DC link is kept at 400 V. The grid receives real power of 2000 W. The overall efficiency of the system is around 95.46 %.

In varying irradiance conditions, various parameters of the PV system are measured and analyzed in figure 7.

From Figure 8, it is observed that power generation from the PV array is around 1047 W, PV panel is around 258 V, and PV current is around 4.05 A. The voltage on the dc-link is kept constant at 400 V. The grid receives real power of 1020 W. The overall efficiency of the system is around 97.42 %.

In varying temperature conditions, the temperature varies from 25°C to 10°C; various parameters of the PV system are measured and analyzed in figure 8.

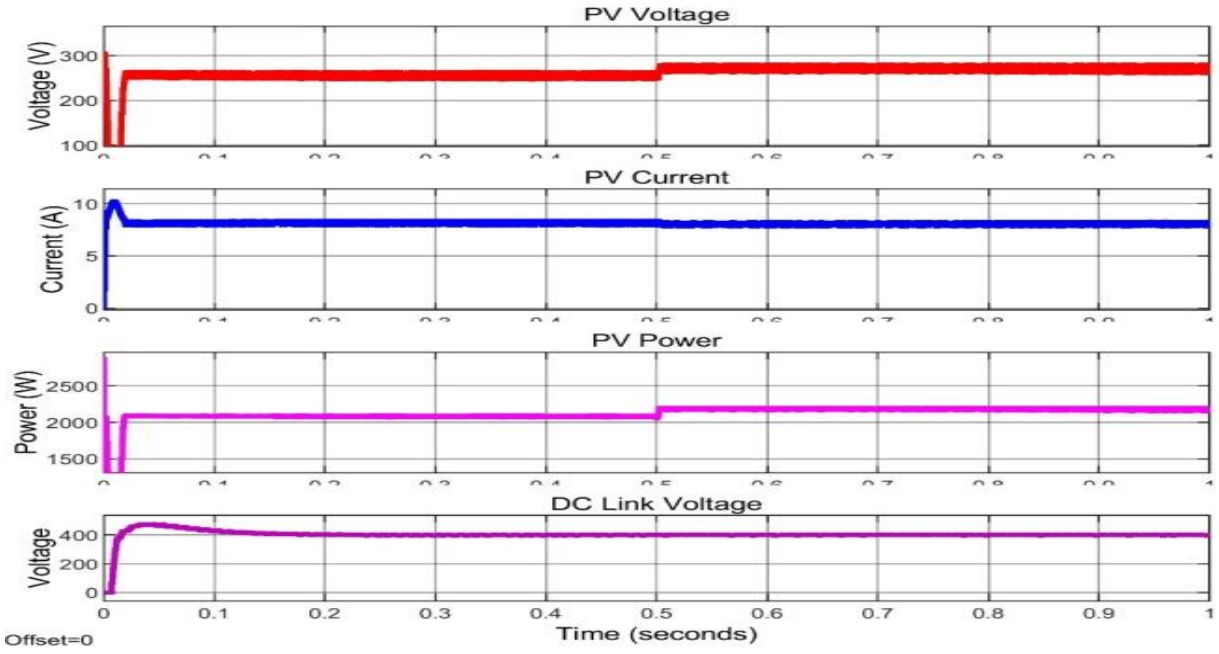

(a)

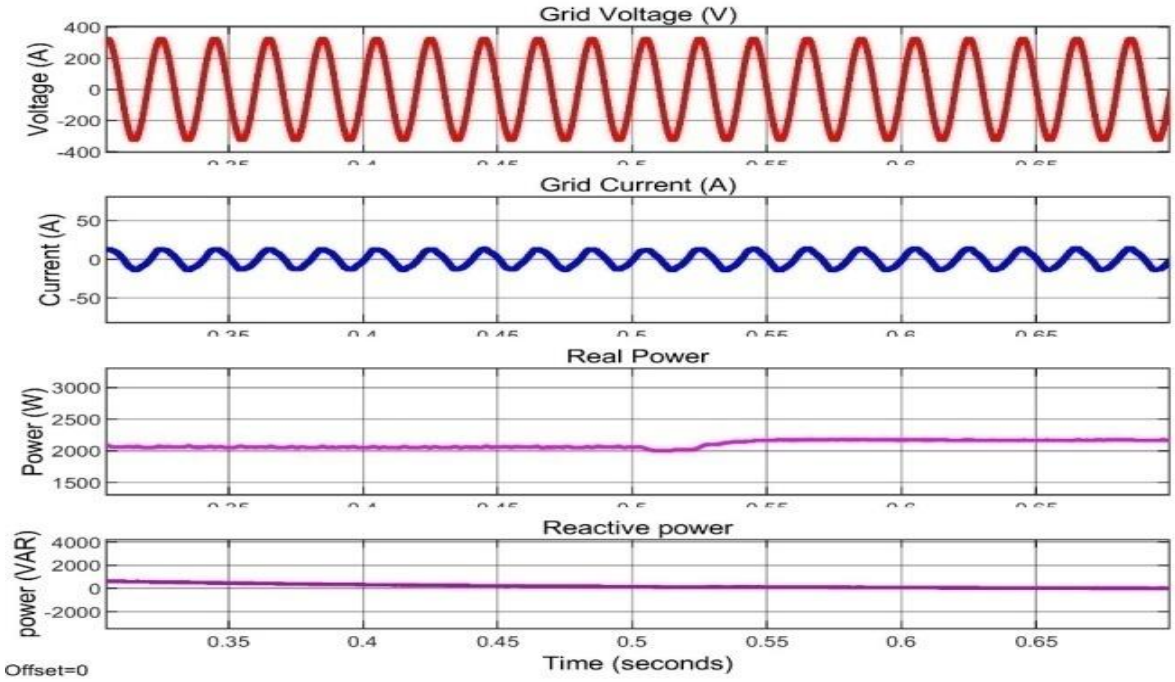

(b)

Fig. 8 Simulation results for varying temperatures from 25°C to 10°C at 0.5 sec: a) PV voltage, current, power, and dc-link voltage, b) Grid voltage, current, real power, and reactive power.

From Figure 8, it is observed that power generation from the PV array is around 2205 W, PV panel is around 270 V, and PV current is around 8.16 A. The voltage on the dc-link is kept constant at 400 V. The grid receives real power of 2180 W. The system has a 98.8% total efficiency. The system is operated under No PV power mode during the nighttime, and the grid inverter system acts as a reactive power compensator. Figure 10 depicts the simulation results for this model.

From figure 9, it is observed that the grid supplies only real power, around 2000 W, the grid inverter is supplying reactive power only, and it is around 1784 var. The planned single-phase grid-connected solar PV system's inverter served as a reactive power compensator during the night.

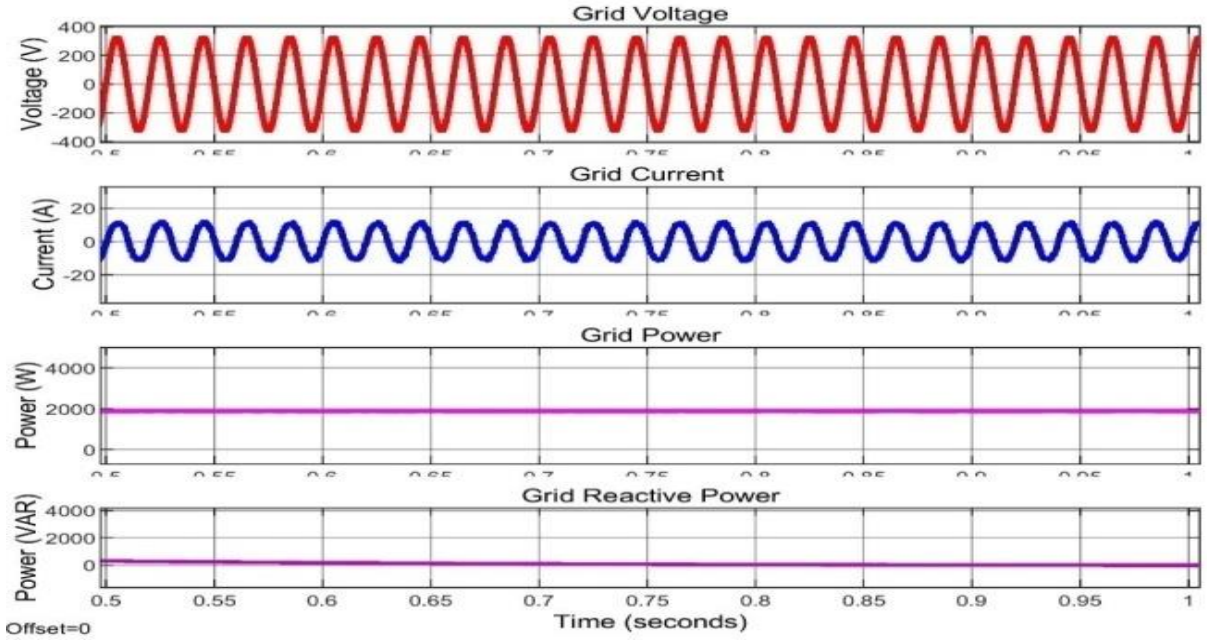

(a)

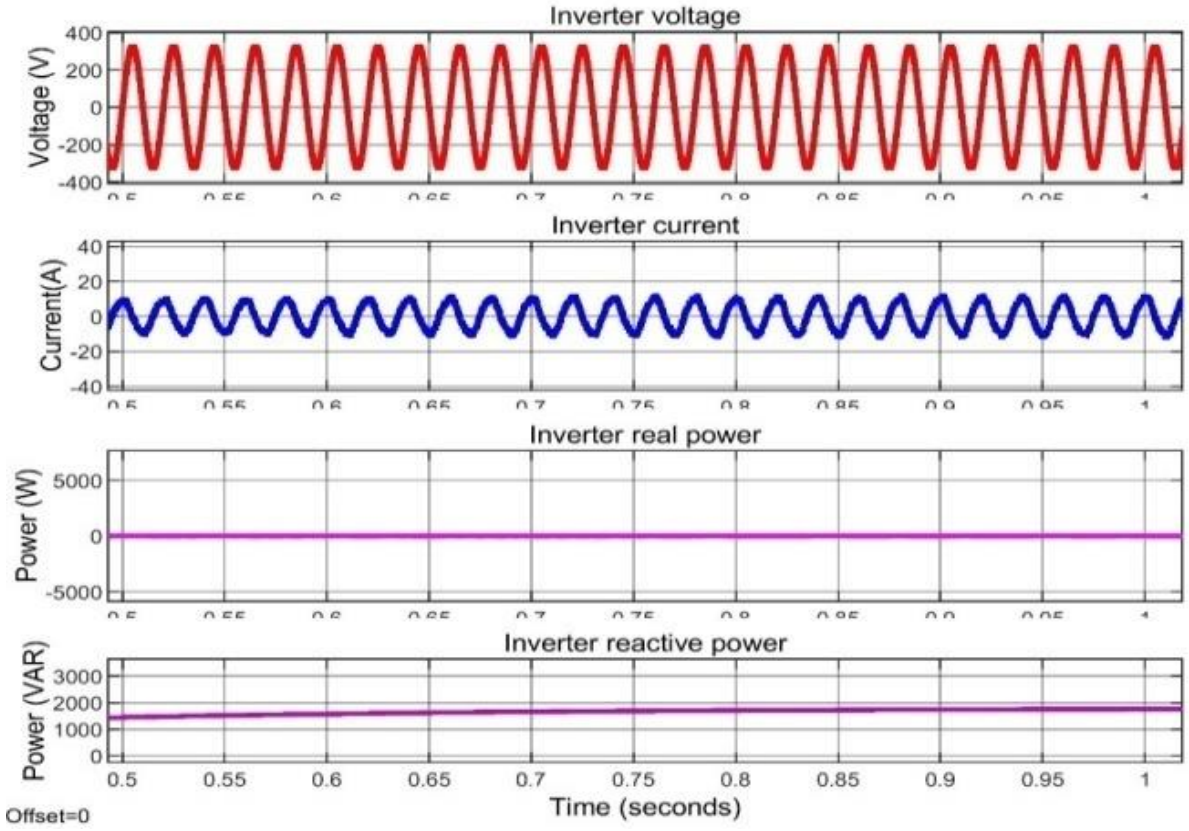

(b)

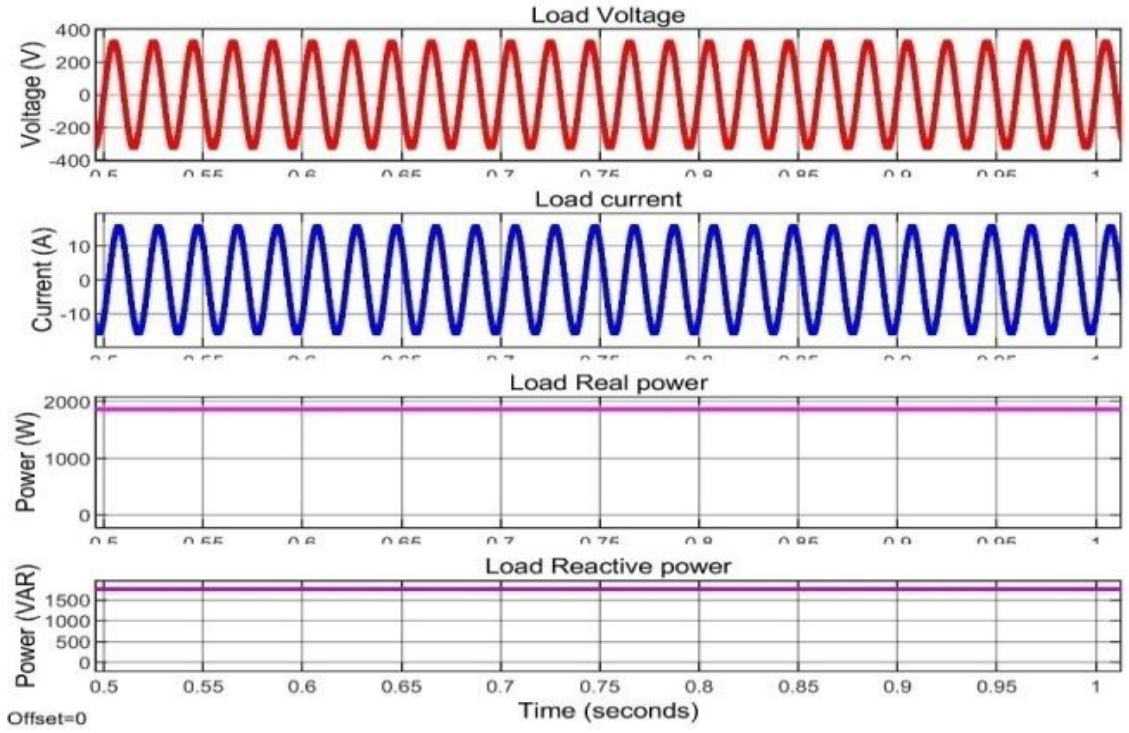

(c)

Fig. 9 Simulation results for No PV Power Mode: a) Grid voltage, grid current, real grid power, and grid reactive power, b) Inverter voltage, inverter current, real inverter power, and reactive inverter power, c) Load voltage, load current, load real power and load reactive power.

5. Conclusion

A double-level system connected to the photovoltaic grid with a coordinated control algorithm is presented. The Perturb & Observe approach using a DC-DC boost converter is employed to keep an eye on the peak power points of a solar photovoltaic system. With two alternative control algorithms, the voltage source inverter can be used in PV power mode and No PV power mode. The voltage source inverter injects real power from the solar PV system into the grid while in PV power mode. The voltage source inverter injects reactive power to compensate for the local load's reactive power needs when no PV power is available. The simulation study is performed using the system proposed in MATLAB Simulink software. The proposed system worked effectively in both modes based on the test results.

Conflicts of Interest

The authors declare that there is no conflict of interest regarding the publication of this article.

References

[1] J. Parikh, K. Parikh, Growing Pains: Meeting India's Energy Needs in the Face of Limited Fossil Fuels, IEEE Power Energy Mag. 10(3) (2012) 59-66.

[2] R. Kadri, J. Gaubert, G. Champenois, An Improved Maximum Power Point Tracking for Photovoltaic Grid-Connected Inverter Based on Voltage-Oriented Control, IEEE Trans. Ind. Electron. 58(1) (2011) 66-75.

[3] B. Singh, M. Kandpal, I. Hussain, Control of Grid Tied Smart PV DSTATCOM System Using an Adaptive Technique, IEEE Trans. Smart Grid. 9(5) (2018) 3986-3993.

[4] N. Kumar, B. Singh, B. K. Panigrahi, LLMLF based Control Approach and LPO MPPT Technique for Improving Performance of a Multifunctional Three-Phase Two-Stage Grid Integrated PV System, IEEE Trans. Sustain. Energy. Doi: 10.1109/TSTE.2019.2891558.

[5] N. R. Tummuru, M. K. Mishra, S. Srinivas, Multifunctional VSC Controlled Microgrid Using Instantaneous Symmetrical Components Theory, IEEE Trans. Sustain. Energy. 5(1) (2014) 313-322.

[6] N. Mahmud, A. Zahedi, and A. Mahmud, A Cooperative Operation of Novel PV Inverter Control Scheme and Storage Energy Management System Based on ANFIS for Voltage Regulation of Grid-Tied PV System, IEEE Trans. Ind. Informat. 13(5) (2017) 2657-2668.

[7] V. T. Tran, K. M. Muttaqi, D. Sutanto, A Robust Power Management Strategy with Multi-Mode Control Features for an Integrated PV and Energy Storage System to Take the Advantage of ToU Electricity Pricing, IEEE Trans. Ind. Appl. 55(2) (2019) 2110-2120.

[8] L. B. G. Campanhol, S. A. O. da Silva, A. A. de Oliveira, V. D. Bacon, Single-Stage Three-Phase Grid-Tied PV System with Universal Filtering Capability Applied to DG Systems and AC Microgrids, IEEE Trans. Power Electron. 32(12) (2017) 9131-9142.

[9] A. Yazdani et al., Modeling Guidelines and a Benchmark for Power System Simulation Studies of Three-Phase Single-Stage Photovoltaic Systems, IEEE Trans. Power Del. 26(2) (2011) 1247-1264.

[10] P. Shah, I. Hussain, B. Singh, A. Chandra, K. Al-Haddad, GI-Based Control Scheme for Single-Stage Grid Interfaced SECS for Power Quality Improvement, IEEE Trans. Ind. Appl. 55(1) (2019) 869- 881.

[11] S. Pradhan, I. Hussain, B. Singh, B. Ketan Panigrahi, Performance Improvement of Grid-Integrated Solar PV System Using DNLMS Control Algorithm, IEEE Trans. Ind. Appl. 55(1) (2019) 78-91.

[12] V. Jain and B. Singh, A Multiple Improved Notch Filter-Based Control for a Single-Stage PV System Tied to a Weak Grid, in IEEE Transactions on Sustainable Energy. 10(1) (2019) 238-247. doi: 10.1109/TSTE.2018.2831704.

[13] Paul Denholm, Robert M. Margolis, Evaluating the Limits of Solar Photovoltaics (PV) in Electric Power Systems Utilizing Energy Storage and Other Enabling Technologies, Energy Policy. 35(9) (2007) 4424-4433.

[14] S. R. Ghatak, S. Sannigrahi and P. Acharjee, Optimised Planning of Power Distribution Network with Solar Energy, Battery Storage and DSTATCOM: A Multi-Objective Approach, IEEE International Conference on Power Electronics, Drives and Energy Systems (PEDES). (2018) 1-6. doi: 10.1109/PEDES.2018.8707636.

[15] N. Korada and M. K. Mishra, Grid Adaptive Power Management Strategy for an Integrated Microgrid with Hybrid Energy Storage, in IEEE Transactions on Industrial Electronics. 64(4) (2017) 2884-2892. doi: 10.1109/TIE.2016.2631443.

[16] S. Kotra, M. K. Mishra, A Supervisory Power Management System for a Hybrid Microgrid with HESS, IEEE Trans. Ind. Electron. 64(5) (2017) 3640-3649.

[17] Y. Riffonneau, S. Bacha, F. Barruel, S. Ploix, Optimal Power Flow Management for Grid Connected PV Systems with Batteries, IEEE Trans. Sustain. Energy. 2(3) (2011) 309-320.

[18] U. Manandhar et al., Energy Management and Control for Grid Connected Hybrid Energy Storage System under Different Operating Modes, in IEEE Transactions on Smart Grid. 10(2) (2019) 1626-1636. doi: 10.1109/TSG.2017.2773643.

[19] H. Kim, B. Parkhideh, T. D. Bongers, H. Gao, Reconfigurable Solar Converter: A Single-Stage Power Conversion PV-Battery System, IEEE Trans. Power Electron. 28(8) (2013) 3788-3797.

[20] CH Venkata Ramesh, A Manjunatha, Compensation of Reactive Power in Grid-Connected Solar PV Array System Using STATCOM and Fixed Capacitor Bank, International Journal of Engineering Trends and Technology. 69(10) (2021) 128-136.

[21] K. K. M. Siu and C. N. M. Ho, Generalized Design Approach of a Family of Grid-Connected Converters Based on Active Virtual Ground Technique for Single-Phase AC Microgrid Applications, in CPSS Transactions on Power Electronics and Applications. 5(3) (2020) 203-212. doi: 10.24295/CPSSTPEA.2020.00017.

[22] J. Xu, Q. Qian, B. Zhang, and S. Xie, Harmonics and Stability Analysis of Single-Phase Grid-Connected Inverters in Distributed Power Generation Systems Considering Phase-Locked Loop Impact, in IEEE Transactions on Sustainable Energy. 10(3) (2019) 1470-1480. doi: 10.1109/TSTE.2019.2893679

[23] Y. Han, H. Chen, Z. Li, P. Yang, L. Xu, and J. M. Guerrero, Stability Analysis for the Grid-Connected Single-Phase Asymmetrical Cascaded Multilevel Inverter with SRF-PI Current Control Under Weak Grid Conditions, in IEEE Transactions on Power Electronics. 34(3) (2019) 2052-2069. doi: 10.1109/TPEL.2018.2867610.

[24] J. Xia, Y. Guo, X. Zhang, J. Jatskevich and N. Amiri, Robust Control Strategy Design for Single-Phase Grid-Connected Converters Under System Perturbations, in IEEE Transactions on Industrial Electronics. 66(11) (2019) 8892-8901. doi: 10.1109/TIE.2019.2902791.

[25] J. Xu, H. Qian, S. Bian, Y. Hu, and S. Xie, Comparative Study of Single-Phase Phase-Locked Loops for Grid-Connected Inverters Under Non-Ideal Grid Conditions, in CSEE Journal of Power and Energy Systems. 8(1) (2022) 155-164. doi: 10.17775/CSEEJPES.2019.02390.

[26] T. Ye, N. Dai, C. S. Lam, M. C. Wong, and J. M. Guerrero, Analysis, Design, and Implementation of a Quasi-Proportional-Resonant Controller for a Multifunctional Capacitive-Coupling Grid-Connected Inverter, IEEE Transactions on Industry Applications. 52 (2016) 4269-4280.

[27] M. Cespedes and J. Sun, Adaptive Control of GridConnected Inverters Based on Online Grid Impedance Measurements, IEEE Transactions on Sustainable Energy. 5 (2014) 516-523.